Fuzzy Adaptive Sliding Mode Control of Fractional-order Chaotic Lorenz Systems

Devasmito Das[1], Ina Taralova[2], and Jean-Jacques Loiseau[3]

Abstract— **This paper proposes a fuzzy adaptive boundary-layer sliding-mode controller for stabilizing fractional-order chaotic Lorenz systems modeled using Grünwald-Letnikov derivatives. The controller combines a fractional-memory sliding surface, adaptive fuzzy gain scheduling, nominal dynamics cancellation, and linear stabilization. Stability is verified using Matignon's criterion, while simulations show convergence to target equilibria, bounded control effort, chattering reduction, and chaos suppression through Lyapunov-exponent analysis.**

Keywords: Fractional-order systems, Sliding mode control, Fuzzy logic, Chaos control, Lyapunov stability, Matignon criterion

I. INTRODUCTION

Fractional-order dynamical systems have gained significant attention as effective models for processes with memory and long-range temporal dependence, arising in viscoelasticity, anomalous diffusion, and biological signal processing [1], [2]. The Lorenz system remains a canonical benchmark for chaotic dynamics and control performance validation [3]. However, extending classical control methodologies to nonlinear fractional-order systems introduces substantial theoretical and computational challenges [18].

Sliding mode control (SMC) is well known for its robustness and finite-time convergence in integer-order systems, yet its application to fractional-order chaotic dynamics remains limited [4], [5]. Moreover, classical SMC suffers from chattering caused by discontinuous control actions, which can degrade performance and excite unmodeled dynamics [6]. Fuzzy logic–based gain adaptation has been shown to mitigate chattering through smooth control modulation [7], but its integration with fractional-order dynamics and rigorous stability guarantees is still underexplored.

Stability analysis of fractional-order systems requires tools beyond standard Lyapunov theory, with the Matignon criterion providing necessary and sufficient conditions for asymptotic stability via eigenvalue argument constraints [8], [9]. However, its systematic use in nonlinear adaptive control remains limited [10]. Existing chaos control approaches often rely on linear or PD-type feedback and assume full-state availability [11], [12], motivating hybrid designs that combine memory-aware sliding surfaces, adaptive gains, and nominal cancellation [19]. To address practical limitations due to partial and noisy measurements, observer-based strategies such as EKF-assisted state estimation for fractional model predictive control have also been investigated [20].

This paper addresses these gaps through a case-study control design for the fractional-order Lorenz benchmark. The proposed controller is not intended as a universal plug-and-play control law for arbitrary nonlinear fractional systems; rather, it illustrates how fractional-memory sliding surfaces, smooth reaching laws, and lightweight adaptive gain scheduling can be combined for a fully actuated chaotic system with matched inputs.

The rest of the paper is organized as follows. Section II presents the fractional-order Lorenz system and its Grünwald–Letnikov discretization. Section III introduces the proposed fuzzy–adaptive sliding-mode controller. Section IV establishes stability using a discrete fractional Lyapunov approach and the Matignon criterion. Section V reports numerical results validating performance and robustness. Section VI concludes the paper and outlines future research directions.

II. PRELIMINARIES

A. Grünwald-Letnikov Fractional Derivative

For a continuous function $f(t)$ and fractional order $\alpha \in (0, 1)$, the GL derivative is defined as [1]:

$$D^{\alpha} f(t) = \lim_{h \to 0^+} \frac{1}{h^{\alpha}} \sum_{j=0}^{\infty} (-1)^j \binom{\alpha}{j} f(t - jh), \qquad (1)$$

where h is the step size and the binomial coefficients encode the fractional memory. With $h = \Delta t$, the discrete GL approximation is [1]:

$$D^{\alpha} f(n) \approx \frac{1}{h^{\alpha}} \sum_{j=0}^{n} w_j^{(\alpha)} f(n - j), \qquad (2)$$

where the binomial coefficients $w_j^{(\alpha)}$ are recursively computed as

$$w_0^{(\alpha)} = 1, \qquad (3)$$

$$w_j^{(\alpha)} = -w_{j-1}^{(\alpha)} \frac{\alpha - (j-1)}{j}, \quad j \geq 1. \qquad (4)$$

The GL weights exhibit alternating signs and algebraic decay, producing the long-memory behavior characteristic of fractional-order systems [1], [2], [17].

[1]Devasmito Das is with École Centrale de Nantes, Nantes Université, LS2N, CNRS, UMR 6004, 1 rue de la Noë, 44321 Nantes, France, and also with the Department of Mechanical Engineering, Indian Institute of Technology Madras, Chennai 600036, India devasmito.das@ls2n.fr

[2]Ina Taralova is with École Centrale de Nantes, Nantes Université, LS2N, CNRS, UMR 6004, 1 rue de la Noë, 44321 Nantes, France ina.taralova@ls2n.fr

[3]Jean-Jacques Loiseau is with École Centrale de Nantes, Nantes Université, LS2N, CNRS, UMR 6004, 1 rue de la Noë, 44321 Nantes, France jean-jacques.loiseau@ls2n.fr

The fractional integral of order $\beta > 0$ is the inverse operation, defined as [1]:

$$I^{\beta} f(t) = \frac{1}{\Gamma(\beta)} \int_0^t (t-\tau)^{\beta-1} f(\tau) d\tau, \tag{5}$$

where $\Gamma(\cdot)$ is the gamma function. In GL discrete form with coefficients $v_j^{(\beta)}$ computed analogously to Eqs. (3)–(4):

$$\begin{aligned} I^{\beta}(n) &= h^{\beta} \sum_{j=1}^{n} v_j^{(\beta)} f(n-j), \\ v_1^{(\beta)} &= 1, \\ v_j^{(\beta)} &= -v_{j-1}^{(\beta)} \frac{\beta-(j-1)}{j}, \qquad j \geq 2. \end{aligned} \tag{6}$$

For the control design in this work, we define $\beta = 1-\alpha$, enabling fractional-order error integration within the sliding surface formulation.

B. Matignon Stability Criterion

For a commensurate (all fractional derivatives in the system have the same order $\alpha \in (0,1)$) fractional-order linear system

$$D^{\alpha}\mathbf{x} = \mathbf{A}\mathbf{x}, \tag{7}$$

the system is asymptotically stable if and only if all eigenvalues λ_i of the system matrix $\mathbf{A}$ satisfy the Matignon criterion [8], [9]:

$$|\arg(\lambda_i)| > \frac{\alpha\pi}{2}. \tag{8}$$

This criterion defines a wedge-shaped stability region in the complex plane. For $\alpha < 1$, the wedge boundary makes an angle of $\alpha\pi/2$ with the positive real axis. Eigenvalues whose arguments satisfy Eq. (8) guarantee exponential decay of perturbations. In the discrete-time setting employed in this work, the criterion applies to the eigenvalues of the Jacobian matrix evaluated at the target equilibrium point.

C. Fractional-Order Lorenz System and Controlled Plant

The fractional-order Lorenz system is defined as:

$$D^{\alpha}x = \sigma(y-x), \tag{9}$$
$$D^{\alpha}y = x(\rho-z)-y, \tag{10}$$
$$D^{\alpha}z = xy-\beta z, \tag{11}$$

The above equations describe the autonomous, uncontrolled plant. In the control problem considered in this paper, the control action is assumed to enter additively through each state equation, yielding the affine controlled fractional-order system

$$D^{\alpha}x = \sigma(y-x)+u_x, \tag{12}$$
$$D^{\alpha}y = x(\rho-z)-y+u_y, \tag{13}$$
$$D^{\alpha}z = xy-\beta z+u_z, \tag{14}$$

where u_x, u_y, u_z are the control inputs to be designed. The control objective is to construct u_x, u_y, u_z such that the state $\mathbf{x} = [x,y,z]^T$ converges to a prescribed equilibrium $\mathbf{x}^*$ while suppressing the chaotic behavior of the uncontrolled fractional-order Lorenz dynamics.

Here, $\mathbf{x} = [x,y,z]^T$, $\alpha \in (0,1)$, and $\sigma > 0$, $\rho > 0$, $\beta > 0$ are the Lorenz parameters. In this work, we employ the classical values $\sigma = 10$, $\rho = 28$, and $\beta = 8/3$. The autonomous system in Eqs. (9)– (11) is used for equilibrium and open-loop stability analysis, while the affine system in Eqs. (12)– (14) is the plant used for controller synthesis.

1) Equilibrium Points of the Uncontrolled System: Setting $D^{\alpha}\mathbf{x} = \mathbf{0}$, the equilibria of the uncontrolled system satisfy:

$$\sigma(y-x) = 0, \tag{15}$$
$$x(\rho-z)-y = 0, \tag{16}$$
$$xy-\beta z = 0. \tag{17}$$

The origin $\mathbf{0} = [0,0,0]^T$ is always an equilibrium. For $\rho > 1$, two additional symmetric non-trivial equilibria exist:

$$\mathbf{E}_{+} = [x_e, x_e, \rho-1]^T, \tag{18}$$
$$\mathbf{E}_{-} = [-x_e, -x_e, \rho-1]^T, \tag{19}$$

where

$$x_e = \sqrt{\beta(\rho-1)} = \sqrt{\frac{8}{3}(28-1)} = \sqrt{72} \approx 8.485. \tag{20}$$

Thus, the non-trivial equilibria are located at approximately $\mathbf{E}_{\pm} = [\pm 8.485, \pm 8.485, 27]^T$ and are unstable. The control objective is to stabilize the system at the positive equilibrium branch $\mathbf{x}^* = \mathbf{E}_{+} = [8.485, 8.485, 27]^T$.

2) Discrete-Time Formulation of the Controlled Plant: Using GL explicit Euler discretization with step size $h = \Delta t = 0.002$, the affine controlled Lorenz dynamics become:

$$x(n) = h^{\alpha}\Big[\sigma\big(y(n-1)-x(n-1)\big)+u_x(n-1)\Big] - \sum_{j=1}^{n-1} w_j^{(\alpha)} x(n-j), \tag{21}$$

$$y(n) = h^{\alpha}\Big[x(n-1)\big(\rho-z(n-1)\big)-y(n-1)+u_y(n-1)\Big] - \sum_{j=1}^{n-1} w_j^{(\alpha)} y(n-j), \tag{22}$$

$$z(n) = h^{\alpha}\Big[x(n-1)y(n-1)-\beta z(n-1)+u_z(n-1)\Big] - \sum_{j=1}^{n-1} w_j^{(\alpha)} z(n-j). \tag{23}$$

For efficient implementation, the GL memory can be truncated to a finite window M [17]:

$$\mathbf{x}(n) \approx h^{\alpha} f(\mathbf{x}(n-1)) - \sum_{j=1}^{\min(n-1,M)} w_j^{(\alpha)} \mathbf{x}(n-j). \tag{24}$$

In the simulations, $M = n-1$ is used, so no truncation error is introduced.

For embedded use, admissible M values follow from the algebraic decay:

$$|w_j^{(\alpha)}| \leq C_{\alpha} j^{-(1+\alpha)}, \qquad j \geq 1,$$

for some constant $C_\alpha > 0$. If the closed-loop trajectory is bounded, i.e. $\|\mathbf{x}(n)\| \le X_{\max}$, then the discarded memory tail is bounded as

$$\|\varepsilon_M(n)\| = \left\| \sum_{j=M+1}^{n-1} w_j^{(\alpha)} \mathbf{x}(n-j) \right\| \le X_{\max} \sum_{j=M+1}^{n-1} |w_j^{(\alpha)}|.$$

Using the integral estimate for the algebraic tail gives

$$\|\varepsilon_M(n)\| \le \frac{C_\alpha X_{\max}}{\alpha} M^{-\alpha}.$$

Therefore, for a prescribed tolerance $\varepsilon_{\mathrm{tol}}$, it is sufficient to choose

$$M \ge \left(\frac{C_\alpha X_{\max}}{\alpha \varepsilon_{\mathrm{tol}}} \right)^{1/\alpha}.$$

Thus, M can be selected from this tail-error bound for embedded implementation.

3) Jacobian and Stability Analysis at $\mathbf{E}_+$: The Jacobian of the autonomous fractional-order Lorenz system at an arbitrary point is

$$\mathbf{J} = \begin{bmatrix} -\sigma & \sigma & 0 \\ \rho - z & -1 & -x \\ y & x & -\beta \end{bmatrix}. \tag{25}$$

Evaluated at the target non-trivial equilibrium $\mathbf{E}_+ = [x_e, x_e, \rho - 1]^T$, with $x_e = 8.485$, $\rho = 28$, $\sigma = 10$, $\beta = 8/3$, and the Jacobian becomes

$$\mathbf{J}_{\mathbf{E}_+} = \begin{bmatrix} -10 & 10 & 0 \\ 1 & -1 & -8.485 \\ 8.485 & 8.485 & -8/3 \end{bmatrix}. \tag{26}$$

Computing the characteristic polynomial and solving for eigenvalues yield: $\lambda_1' \approx -11.826, \quad \lambda_{2,3}' \approx 0.413 \pm 10.195i$.

The eigenvalues $\lambda_{2,3}'$ have positive real parts and violate Matignon's criterion for $\alpha = 0.995$, since $|\arg(\lambda_{2,3}')| \approx 87.7^\circ < \alpha\pi/2 \approx 89.5^\circ$. Hence, the equilibrium $\mathbf{E}_+$ is unstable in the uncontrolled fractional-order Lorenz system. The control objective is therefore to design the additive inputs u_x, u_y, u_z in Eqs. (12)–(14) so that $\mathbf{x} \to \mathbf{x}^*$, $s_i \to 0$, and the closed-loop eigenvalues lie inside the Matignon-stable region.

III. Control Law Design

This section designs the inputs u_x, u_y, u_z for the affine plant in Eqs. (12)–(14). The controller combines a GL memory-based sliding surface, adaptive fuzzy reaching law, linear stabilization, and nominal dynamics cancellation to stabilize the fractional-order Lorenz system.

A. Sliding Surface Construction with Memory-Dependent Fractional Integral

1) Motivation and Design Principle: Classical integer-order sliding mode control uses surfaces such as

$$s_i = e_i + \eta_i \dot{e}_i, \tag{27}$$

where $e_i = x_i - x_i^*$. However, this form only captures instantaneous error and rate information. For the fractional-order Lorenz system $D^\alpha \mathbf{x} = \mathbf{f}(\mathbf{x})$, the dynamics include power-law memory through the GL convolution, making a memory-dependent sliding surface more appropriate.

Hence, we propose a **commensurate sliding surface** that respects the system's fractional-order nature:

$$s_i(n) = e_i(n) + \eta_i I_i^{1-\alpha}(n), \tag{28}$$

where $e_i(n) = x_i(n) - x_i^*$, $\eta_i > 0$ is the sliding coefficient, and $I_i^{1-\alpha}(n)$ is the GL fractional integral of the error. In the simulations, $\eta_i = 0.8$, $\alpha = 0.995$, and $1 - \alpha = 0.005$.

2) Fractional Integral Computation: The fractional integral of error is computed as [1], [2]:

$$I_i^{1-\alpha}(n) = h^{1-\alpha} \sum_{m=1}^{n-1} v_m^{(1-\alpha)} \cdot e_i(n-m), \tag{29}$$

where $h = \Delta t = 0.002$ s and the GL integral coefficients $v_m^{(\beta)}$ with $\beta = 1 - \alpha = 0.005$ are recursively defined:

$$v_1^{(1-\alpha)} = 1, \tag{30}$$

$$v_m^{(1-\alpha)} = -v_{m-1}^{(1-\alpha)} \cdot \frac{(1-\alpha) - (m-1)}{m}, \quad m = 2, 3, \ldots \tag{31}$$

3) Physical and Mathematical Interpretation: When $s_i = 0$, the error satisfies $e_i(n) = -\eta_i I_i^{1-\alpha}(n)$, so the sliding manifold preserves the GL memory structure through algebraically weighted past errors [1], [2].

B. Adaptive Fuzzy Reaching Law Synthesis

1) Motivation for Lightweight Fuzzy Logic: Traditional Takagi–Sugeno fuzzy SMC often requires multi-rule linearization and LMI-based tuning, increasing computational cost [4], [6]. Here, a lightweight three-level adaptive fuzzy gain is used to retain robustness while remaining compatible with explicit GL discretization [10], [13], [16].

2) Fuzzy Gain Definition: The adaptive fuzzy gain is defined as a three-level, piecewise-constant function of the sliding surface magnitude $|s_i|$:

$$K_i(|s_i|) = \begin{cases} K_{\mathrm{min}} = 0.5 & \text{if } |s_i| < \epsilon_1 = 0.05, \\ K_{\mathrm{mid}} = 1.5 & \text{if } \epsilon_1 \le |s_i| < \epsilon_2 = 0.3, \\ K_{\mathrm{max}} = 3.0 & \text{if } |s_i| \ge \epsilon_2. \end{cases} \tag{32}$$

Interpretation: The gain scheduling assigns low gains near the equilibrium to reduce chattering, moderate gains for intermediate errors to balance transients, and high gains for large deviations to ensure fast reaching and strong disturbance rejection, thereby increasing control authority with error magnitude while maintaining smooth convergence near the target.

3) Fuzzy Reaching Law: The fuzzy-based reaching law for the sliding surface is:

$$u_{i,\mathrm{fuzz}} = -K_i(|s_i|) \cdot \tanh(s_i), \tag{33}$$

where $K_i(|s_i|)$ is the adaptive gain and $\tanh(s_i)$ provides smooth bounded saturation.

The fuzzy rule in Eq. (33) is used as a lightweight gain-scheduling mechanism rather than a Takagi–Sugeno fuzzy model. Hence, no LMI-based optimality or global fuzzy-model stability claim is made. Its role is to increase the reaching gain for large sliding errors and reduce it near the equilibrium to limit chattering and control effort.

Compared with the discontinuous sign function, $\tanh(\cdot)$ gives a bounded and smooth correction, reducing chattering and improving numerical implementation.

C. Three-Part Control Architecture

For each state, the control input is decomposed as

$$u_i(n) = u_{i,\text{nom}}(n) + u_{i,\text{lin}}(n) + u_{i,\text{fuzz}}(n). \tag{34}$$

The design assumes a fully actuated matched-input benchmark; underactuated, partial-state, and cancellation-free robust designs are left for future work.

1) Part (A): Linear Stabilization Gains:

$$u_{i,\text{lin}} = -k_i(x_i(n) - x_i^*), \tag{35}$$

where $k_i > 0$ are linear feedback gains selected within the Matignon-stable region. For the reduced dynamics $D^\alpha e_i = -k_i e_i$, the eigenvalues are $\lambda_i = -k_i$, so $|\arg(\lambda_i)| = \pi > \alpha\pi/2$ for all $\alpha \in (0,1)$. The values $k = [15, 15, 12]^T$ are chosen to obtain a suitable transient response with bounded control effort, while $x_i(n) - x_i^*$ denotes the state error.

2) Part (B): Nominal Dynamics Cancellation: Since the controlled plant in Eqs. (12)–(14) is affine in the inputs, the nominal nonlinear vector field can be compensated through the model-based term

$$u_{x,\text{nom}} = -\sigma\big(y(n) - x(n)\big), \tag{36}$$
$$u_{y,\text{nom}} = -\big[x(n)(\rho - z(n)) - y(n)\big], \tag{37}$$
$$u_{z,\text{nom}} = -\big[x(n)y(n) - \beta z(n)\big]. \tag{38}$$

This cancellation is used here for the fully actuated benchmark case. The remaining terms provide error stabilization and smooth reaching dynamics.

D. Complete Control Law

The complete control input is written explicitly as

$$\begin{aligned} u_x(n) = &-\sigma\big(y(n) - x(n)\big) \\ &- k_1\big(x(n) - x^*\big) \\ &- K_1(|s_1|)\tanh(s_1(n)), \end{aligned} \tag{39}$$

$$\begin{aligned} u_y(n) = &-\big[x(n)(\rho - z(n)) - y(n)\big] \\ &- k_2\big(y(n) - y^*\big) \\ &- K_2(|s_2|)\tanh(s_2(n)), \end{aligned} \tag{40}$$

$$\begin{aligned} u_z(n) = &-\big[x(n)y(n) - \beta z(n)\big] \\ &- k_3\big(z(n) - z^*\big) \\ &- K_3(|s_3|)\tanh(s_3(n)). \end{aligned} \tag{41}$$

E. Closed-Loop System Dynamics

Substituting Eqs. (39)–(41) into Eqs. (12)–(14) yields the closed-loop error dynamics

$$D^\alpha e_x(n) = -k_1 e_x(n) - K_1(|s_1|)\tanh(s_1(n)), \tag{42}$$
$$D^\alpha e_y(n) = -k_2 e_y(n) - K_2(|s_2|)\tanh(s_2(n)), \tag{43}$$
$$D^\alpha e_z(n) = -k_3 e_z(n) - K_3(|s_3|)\tanh(s_3(n)). \tag{44}$$

The nominal nonlinearities are compensated in the fully actuated benchmark, and the remaining closed-loop dynamics are expressed directly in terms of the tracking errors.

Key observation: The closed-loop decouples into three fractional-order subsystems, each with negative-definite control, ensuring convergence to equilibrium [8], [9].

F. Discrete-Time Implementation Algorithm

Algorithm 1 Discrete-Time Control Loop for Fractional-Order Lorenz System

Require: $x(n-1), y(n-1), z(n-1)$, target equilibrium $x^* = y^* = 8.485$, $z^* = 27$
Ensure: Control inputs $u_x(n), u_y(n), u_z(n)$
Step 1: Compute error components
$e_x(n) \leftarrow x(n-1) - x^*$, $e_y(n) \leftarrow y(n-1) - y^*$, $e_z(n) \leftarrow z(n-1) - z^*$
Step 2: Update fractional integral of error
for $m = 1$ to $\min(n-1, M)$ **do**
    $I_x^{1-\alpha} \leftarrow I_x^{1-\alpha} + v_m^{(0.005)} \cdot e_x(n-m)$
    $I_y^{1-\alpha} \leftarrow I_y^{1-\alpha} + v_m^{(0.005)} \cdot e_y(n-m)$
    $I_z^{1-\alpha} \leftarrow I_z^{1-\alpha} + v_m^{(0.005)} \cdot e_z(n-m)$
end for
Scale by $h_\beta = (0.002)^{0.005}$
Step 3: Compute sliding surfaces
$s_1(n) \leftarrow e_x(n) + 0.8 \cdot I_x^{1-\alpha}$, and similarly for s_2, s_3
Step 4: Compute adaptive fuzzy gains based on $|s_i|$ thresholds
Step 5: Compute control inputs using Eqs. (39)–(41)
return $u_x(n), u_y(n), u_z(n)$

For the numerical results in Section V, Algorithm 1 is evaluated in the full-memory configuration by taking $M = n-1$. The notation $\min(n-1, M)$ is kept to show the general implementation form, where a smaller M may be selected according to the truncation-error bound derived in Section II.

IV. Stability Analysis

This section provides rigorous stability verification using three complementary tools: (i) a fractional Lyapunov argument, (ii) Matignon's eigenvalue criterion, and (iii) a convergence synthesis combining both.

A. Discrete Fractional Lyapunov Analysis

Consider the sliding energy function

$$V(n) = \frac{1}{2}\sum_{i=1}^{3} s_i^2(n). \tag{45}$$

Using the smooth reaching term

$$u_{i,\text{fuzz}} = -K_i(|s_i|)\tanh(s_i), \tag{46}$$

with $K_i(|s_i|) \geq K_{\min} > 0$, the product $s_i \tanh(s_i)$ is non-negative for all s_i. Therefore, in the nominal case, the reaching term is dissipative and yields

$$\Delta V(n) \leq -K_{\min} \sum_{i=1}^{3} |s_i(n)|\,|\tanh(s_i(n))|. \tag{47}$$

Because $\tanh(s_i)$ is continuous, the controller is interpreted as a boundary-layer SMC rather than an ideal discontinuous SMC; therefore, finite-time ideal sliding is not claimed. In the nominal case, the smooth reaching term and linear feedback ensure asymptotic decay, while bounded disturbances lead to practical convergence or uniform ultimate boundedness.

Since $V(n)$ is positive definite and non-increasing, the sliding variables remain bounded and are driven toward $s_i = 0$. On this manifold, the reduced fractional error dynamics satisfy Matignon's criterion, ensuring asymptotic stability of the equilibrium.

B. Linearization and Matignon Criterion

Once on the sliding manifold, the linearized fractional error dynamics reduce to $D^{\alpha} e_i(n) \approx -k_i e_i(n)$, yielding eigenvalues $\lambda_i = -k_i$. For $\alpha = 0.995$, Matignon's criterion requires $|\arg(\lambda_i)| > \alpha\pi/2 \approx 89.51°$, which is satisfied for all closed-loop eigenvalues, providing an approximate $53°$ robustness margin and admissible gains down to $k_{\min} = 12$. Numerical simulations confirm stability, with the tracking error converging to $|e| < 10^{-3}$ within $4\,\text{s}$ and the maximum Lyapunov exponent decreasing from 0.756367 to $\lambda_{\max} \approx -1.17 \times 10^{-3}$.

C. Convergence Synthesis

A discrete fractional Lyapunov argument ensures a monotonic decrease of $V(n)$ in the nominal case and drives the sliding variables toward a small boundary layer around $s_i = 0$. The use of $\tanh(s_i)$ avoids chattering but replaces ideal finite-time sliding by smooth practical reaching. Once on the sliding manifold, the closed-loop eigenvalues satisfy Matignon's criterion with a large stability margin, yielding fractional-order exponential decay and asymptotic convergence of the trajectories to the equilibrium $\mathbf{x}^*$ from arbitrary initial conditions.

D. Robustness to Uncertainties

For bounded uncertainties satisfying $\|\Delta(n)\| + \|\mathbf{d}(n)\| \leq 0.15$, the fuzzy gain scheduling improves robustness while keeping the control bounded [5], [11], [12]. The low gain $K_{\min} = 0.5$ reduces chattering near the sliding manifold, whereas $K_{\max} = 3.0$ strengthens correction during large-error transients, with $|u_{i,\text{fuzz}}| \leq K_{\max}$. The thresholds $\epsilon_1 = 0.05$ and $\epsilon_2 = 0.3$ define the gain regions; their systematic optimization is left for future work.

V. Simulation Results and Experimental Validation

The controller is simulated for $N = 15000$ samples with $\Delta t = 0.002\,\text{s}$ using full GL memory $M = n - 1$. The figures focus on the transient interval, where convergence and control activity are most visible.

A. Phase Portrait and Trajectory Convergence

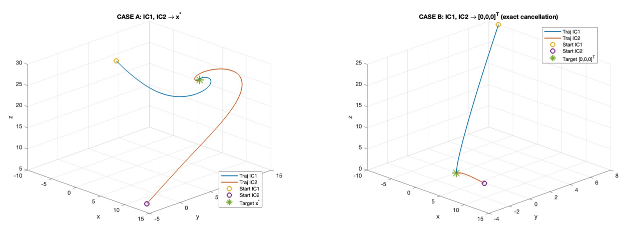

(a) Convergence to $\mathbf{E}_+$ (b) Convergence to the origin

Fig. 1: Closed-loop phase portraits from different initial conditions.

Figure 1 shows 3D phase portraits where trajectories starting from $[-8, 8, 25]^T$ and $[12, -3, 5]^T$ converge smoothly to the target equilibrium and the origin. The results indicate set-point–independent stabilization with chattering-free, $\tanh$-saturated control and convergence within 5–10 s.

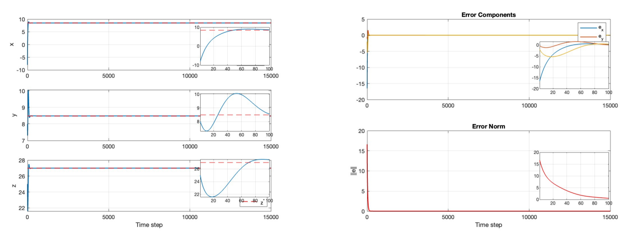

(a) State trajectories (b) Error trajectories

Fig. 2: State and error dynamics under fuzzy–sliding control.

Figure 2a shows the state evolution over the transient interval, where all states rapidly converge from chaotic initial conditions to the target equilibrium. The shortened time axis emphasizes the effective convergence process instead of the uninformative steady-state portion after settling. Transients decay rapidly, after which the system settles smoothly on the sliding manifold with negligible steady-state error.

Figure 2b shows errors converging rapidly: the norm drops from ~ 16.8 to < 0.5 in 2 s and below 10^{-3} after 10 s, following fractional-order decay $|\mathbf{e}(t)| \sim t^{-0.995}$.

Figure 3a shows bounded initial transients (50–100 steps) with $|u_{i,\text{fuzz}}| \leq K_{\max}$; signals smooth after 0.1 s and decay near zero by 4 s with no chattering.

B. Matignon Stability Verification and Eigenvalue Analysis

Figure 3b verifies Matignon stability for $\alpha = 0.995$. The uncontrolled complex pair $\lambda'_{2,3} \approx 0.413 \pm 10.195i$ violates the criterion since $|\arg(\lambda'_{2,3})| \approx 87.7° < 89.5°$. Under control, all closed-loop eigenvalues satisfy $|\arg(\lambda_{c,i})| \approx$

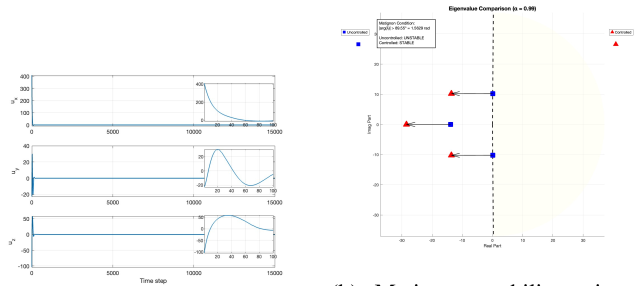

(a) Control inputs

(b) Matignon stability: eigenvalue placement

Fig. 3: Control effort and stability verification.

$143.02^\circ > 89.55^\circ$, giving a robustness margin of about 53.47°.

C. Robustness and Uncertainty Analysis

Additional robustness simulations were performed with parameter mismatch and bounded disturbances. The controller was designed with nominal parameters $(\sigma, \rho, \beta) = (10, 28, 8/3)$, while the plant used $\sigma_p = 1.1\sigma$, $\rho_p = 0.9\rho$, $\beta_p = 1.1\beta$, and $d_i(t) = 0.05\sin(2t)$, $i = x, y, z$. The closed-loop trajectories remained bounded and converged to a small neighborhood of the target equilibrium, with slightly increased settling time and a small residual error, consistent with the smooth boundary-layer reaching law. From an implementation viewpoint, the controller is digitally realizable through explicit GL convolution; using a finite memory length M, the cost is $O(M)$ per state, while fuzzy gain evaluation requires only threshold comparisons.

D. Applications and Limitations

The framework is relevant for fractional-order circuits, chaotic secure communication, viscoelastic vibration attenuation, and hereditary biological models. However, it is developed for a fully actuated matched-input Lorenz benchmark; underactuation, actuator limits, partial measurements, and experimental validation remain future work.

VI. Conclusion and Future Scope

A GL-based fuzzy boundary-layer sliding controller was developed for a fully actuated fractional-order Lorenz benchmark. The method combines memory-dependent sliding surfaces, lightweight fuzzy gain scheduling, nominal cancellation, and Matignon-based stability verification. Simulations confirmed convergence, bounded control, chattering reduction, and chaos suppression. Future work will address underactuated systems, observer-based implementation, actuator constraints, and experimental validation.

ACKNOWLEDGMENT

We would like to convey our gratitude to École Centrale de Nantes and IIT Madras for the provided research opportunity.

References

[1] I. Podlubny, *Fractional Differential Equations: An Introduction to Fractional Derivatives, Fractional Differential Equations, Methods of Their Solution and Some of Their Applications*, Vol. 198. Amsterdam: Elsevier, 1998.

[2] A. A. Kilbas, H. M. Srivastava, and J. J. Trujillo, *Theory and Applications of Fractional Differential Equations*, Vol. 204. Amsterdam: Elsevier, 2006.

[3] E. N. Lorenz, *Deterministic Nonperiodic Flow*, in *Universality in Chaos*, 2nd ed., pp. 367–378. London: Routledge, 2017.

[4] V. Utkin, *Variable Structure Systems with Sliding Modes*, *IEEE Transactions on Automatic Control*, vol. 22, no. 2, pp. 212–222, 2003.

[5] H. T. Yau, C. O. K. Chen, and C. L. Chen, *Sliding Mode Control of Chaotic Systems with Uncertainties*, *International Journal of Bifurcation and Chaos*, vol. 10, no. 5, pp. 1139–1147, 2000.

[6] K. D. Young, V. I. Utkin, and U. Ozguner, *A Control Engineer's Guide to Sliding Mode Control*, *IEEE Transactions on Control Systems Technology*, vol. 7, no. 3, pp. 328–342, 1999.

[7] A. Boulkroune, A. Bouzeriba, and A. Boubellouta, *Fuzzy sliding mode control based fast finite-time projective synchronization for fractional-order chaotic systems*, *Archives of Control Sciences*, vol. 34, no. 3, pp. 473–500, 2024.

[8] D. Matignon, *Stability Results for Fractional Differential Equations with Applications to Control Processing*, in *Computational Engineering in Systems Applications*, vol. 2, no. 1, pp. 963–968, Jul. 1996.

[9] M. S. Tavazoei and M. Haeri, *A Note on the Stability of Fractional Order Systems*, *Mathematics and Computers in Simulation*, vol. 79, no. 5, pp. 1566–1576, 2009.

[10] N. Turab et al., *Adaptive sliding mode control for chaotic system synchronization using neural networks*, *Scientific Reports*, vol. 15, no. 1, p. 37547, 2025.

[11] R. Liu et al., *Adaptive fuzzy command filtered control for uncertain fractional-order nonlinear systems with full-state constraints*, *Scientific Reports*, vol. 15, no. 1, 2025.

[12] J. G. Lu and Y. Chen, *Stability and Stabilization of Fractional-Order Linear Systems with Convex Polytopic Uncertainties*, *Fractional Calculus and Applied Analysis*, vol. 16, no. 1, pp. 142–157, 2013.

[13] A. Razzaghian, R. Kardehi Moghaddam, and N. Pariz, *Adaptive fuzzy fractional-order nonsingular fast terminal sliding mode control*, *Mechanical Systems and Signal Processing*, vol. 5, no. 1, pp.77-87, 2022.

[14] K. Khettab, S. Ladaci, and Y. Bensafia, *Fuzzy Adaptive Control of Fractional Order Chaotic Systems with Unknown Control Gain Sign Using a Fractional Order Nussbaum Gain*, *IEEE/CAA Journal of Automatica Sinica*, vol. 6, no. 3, pp. 816–823, 2016.

[15] T. T. Hartley, C. F. Lorenzo, and H. K. Qammer, *Chaos in a Fractional Order Chua's System*, *IEEE Transactions on Circuits and Systems I: Fundamental Theory and Applications*, vol. 42, no. 8, pp. 485–490, 1995.

[16] C. Luo and X. Wang, *Chaos in the Fractional-Order Complex Lorenz System and Its Synchronization*, *Nonlinear Dynamics*, vol. 71, no. 1, pp. 241–257, 2013.

[17] K. Diethelm, N. J. Ford, and A. D. Freed, *A Predictor-Corrector Approach for the Numerical Solution of Fractional Differential Equations*, *Nonlinear Dynamics*, vol. 29, no. 1, pp. 3–22, 2002.

[18] D. Das, I. Taralova, J.-J. Loiseau, and S. Filipova-Petrakieva, *Fractional Model Predictive Control of Fractional Chaotic Rössler Oscillator*, *IFAC-PapersOnLine*, vol. 59, no. 11, pp. 156–161, 2025.

[19] D. Das, I. Taralova, T. Slavov, J.-J. Loiseau, and M. Pandey, *An Active Control Scheme Implemented Via Nonlinear Feedback Linearization for Coupled Fractional-Order Rössler Oscillators: Two and Three Oscillator Configurations*, in *Proc. 2025 Int. Conf. Automatics, Robotics and Artificial Intelligence (ICARAI)*, pp. 1–6, IEEE, June 2025.

[20] D. Das, I. Taralova, J.-J. Loiseau, and T. Slavov, *State Estimation using Extended Kalman Filter for Fractional Model Predictive Control of Fractional Chaotic Rössler Oscillator*, in *Proc. 2025 11th Int. Conf. Control, Decision and Information Technologies (CoDIT)*, vol. 1, pp. 1530–1535, IEEE, July 2025.